

Bulk antiferromagnetism in  $\text{Na}_{0.82}\text{CoO}_2$  single crystalsS. P. Bayrakci,<sup>1</sup> C. Bernhard,<sup>1</sup> D. P. Chen,<sup>1</sup> B. Keimer,<sup>1</sup> R. K. Kremer,<sup>1</sup> P. Lemmens,<sup>1</sup> C. T. Lin,<sup>1</sup> C. Niedermayer,<sup>2</sup> and J. Stropfer<sup>1</sup><sup>1</sup>Max Planck Institute for Solid State Research, Heisenbergstrasse 1, D-70569 Stuttgart, Germany<sup>2</sup>Paul-Scherrer-Institut, CH-5232 Villigen, Switzerland

(Received 15 December 2003; published 25 March 2004)

Susceptibility, specific heat, and muon spin rotation measurements on high-quality single crystals of  $\text{Na}_{0.82}\text{CoO}_2$  have revealed bulk antiferromagnetism with Néel temperature  $T_N = 19.8 \pm 0.1$  K and an ordered moment perpendicular to the  $\text{CoO}_2$  layers. The magnetic order encompasses nearly 100% of the crystal volume. The susceptibility exhibits a broad peak around 30 K, characteristic of two-dimensional antiferromagnetic fluctuations. The in-plane resistivity is metallic at high temperatures and exhibits a minimum at  $T_N$ .

DOI: 10.1103/PhysRevB.69.100410

PACS number(s): 75.30.-m, 76.75.+i, 72.80.Ga, 71.30.+h

Long-standing interest in the interplay between spin, charge, and orbital degrees of freedom in cobalt oxides has increased following the recent discovery of superconductivity at  $T_c = 4.6$  K in the hydrated cobaltate  $\text{Na}_{0.35}\text{CoO}_2 \cdot 1.3 \text{H}_2\text{O}$  (Ref. 1). The triangular  $\text{CoO}_2$  layers of  $\text{Na}_x\text{CoO}_2$  are isostructural to those of  $\text{Na}_{0.35}\text{CoO}_2 \cdot 1.3 \text{H}_2\text{O}$  (Refs. 2–4). It may therefore serve as a reference system with respect to the effects of doping and magnetic correlations.  $\text{Na}_x\text{CoO}_2$  is metallic<sup>5</sup> and exhibits an unusual Hall effect,<sup>6</sup> as well as a very large thermopower.<sup>7</sup> The thermopower increases with increasing  $x$  (Ref. 8), which in a local-moment picture corresponds to a progressive dilution of magnetic  $\text{Co}^{4+}$  ( $S=1/2$ ) with nonmagnetic  $\text{Co}^{3+}$  ( $S=0$ ). Following observations of a pronounced field dependence, a magnetic mechanism has been invoked to explain the large thermopower.<sup>6</sup> It is therefore important to determine the magnetic ground state and exchange parameters in this material. We have taken an important step in this direction by synthesizing high-quality single crystals of  $\text{Na}_x\text{CoO}_2$  with  $x \sim 0.8$  and studying their resistivity, specific heat, and magnetic susceptibility as a function of temperature.

Cylindrical single crystals of diameter 6 mm and length 80 mm were grown in an optical floating-zone furnace. The initial polycrystalline material was prepared using a mixture of  $\text{Na}_2\text{CO}_3$  and  $\text{Co}_3\text{O}_4$  with a Na:Co ratio of 0.8:1. The powders were calcined at  $750^\circ\text{C}$  for 12 h and then reacted at  $850^\circ\text{C}$  for a day with intermediate grindings. The mixture was pressed to form a cylinder and premelted prior to growth. The molten zone was passed through the feed rod under oxygen flow at a rate of 2 mm/h. Details will be published elsewhere.<sup>9</sup> Pieces cut from two of the resulting crystals were analyzed by inductively coupled plasma atomic emission spectroscopy and atomic absorption spectroscopy. The Na:Co ratios were found to be  $0.82 \pm 0.02$  and  $0.83 \pm 0.02$ , respectively. The virtually identical compositions attest to good reproducibility of the crystal preparation. The Néel temperatures of both samples were also identical, within experimental error. Single-crystal and powder x-ray diffraction reveal the nearly pure  $\gamma$  crystallographic phase with space group  $P6_3/mmc$ , in good agreement with Refs. 2 and 4 and with Raman-scattering experiments.<sup>10</sup> The lattice parameters were determined by single-crystal x-ray diffraction along  $(h, h, 0)$  and  $(0, 0, l)$  at room temperature, resulting

in values of  $a = 2.843(1)$  Å and  $c = 10.687(5)$  Å. The susceptibility, specific heat, and resistivity measurements were carried out in Quantum Design MPMS and PPMS systems.

Figure 1 shows the magnetic susceptibility measured in a 5 T magnetic field oriented either along the  $c$  axis or perpendicular to it. Upon cooling, the anisotropy increases, and a broad peak develops around  $31 \pm 3$  K. This is indicative of short-range, Ising-type, quasi-two-dimensional antiferromagnetic correlations. A sharp decrease of the  $c$ -axis susceptibility around 20 K heralds an antiferromagnetic transition with ordered moments along  $c$ . The inset in Fig. 1 shows that the transition is sharp and only weakly affected by the field. Curie tails, presumably due to paramagnetic impurities, are suppressed in a 5 T field.

Mikami *et al.* observed an antiferromagnetic transition at 20 K in a single crystal with  $x = 0.9$  (Ref. 11).  $\text{Na}_x\text{CoO}_2$  with this sodium content crystallizes in the  $\alpha$  phase, which differs

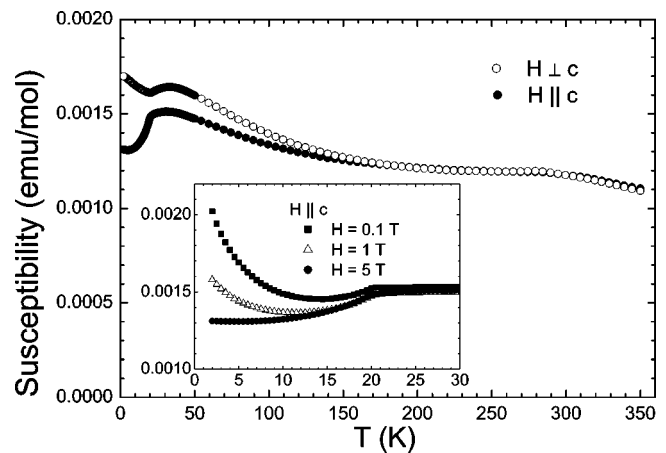


FIG. 1. Magnetic susceptibility of  $\text{Na}_{0.82}\text{CoO}_2$  measured on cooling in a 5 T magnetic field oriented along (open symbols) and perpendicular to (closed symbols) the  $c$  axis. The molar susceptibility measured in other samples from the same ingot is smaller, differing by up to 0.0006 emu/mol. The variation as a function of temperature is closer to a constant offset than to a scale factor. The antiferromagnetic transition occurs at the same temperature in all samples measured. Inset: Low-temperature susceptibility along  $c$  in different applied fields.

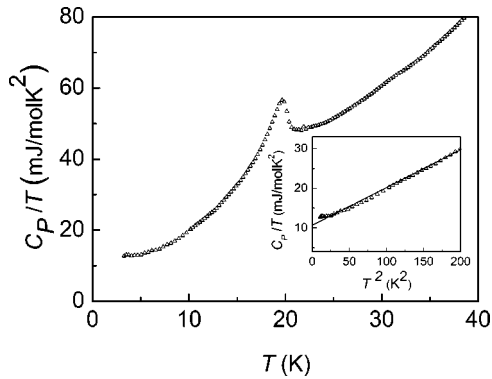


FIG. 2. Specific heat of a  $\text{Na}_{0.82}\text{CoO}_2$  crystal. Inset: Low-temperature specific heat in a  $C_p/T = \gamma + \beta T^2$  plot.

from the  $\gamma$  phase in the stacking pattern of the  $\text{CoO}_2$  layers.<sup>2</sup> The coordination of the sodium ions is correspondingly different. That the antiferromagnetic transition occurs at the same temperature in both phases suggests that the details of the three-dimensional arrangement of the  $\text{CoO}_2$  layers have little influence on the magnetic behavior, and that this behavior is determined by the two-dimensional layers themselves.

In magnetic susceptibility measurements on  $\gamma$ -phase  $\text{Na}_x\text{CoO}_2$  powder samples with  $x=0.75$ , Motohashi *et al.* observed hysteresis between zero-field-cooled and field-cooled sweeps below 22 K (Ref. 12). This hysteresis increased with decreasing temperature; the maximal concomitant spontaneous magnetization was roughly  $10^{-4} \mu_B/\text{Co}^{4+}$  site at 2 K. In contrast, we observe a much smaller hysteresis which develops below  $\sim 250$  K and increases slowly with decreasing temperature. However, this hysteresis decreases rapidly as the temperature drops below  $T_N$ , and at 4.5 K is smaller than our measurement uncertainty. At its maximum, the hysteresis in our measured magnetization is roughly two orders of magnitude smaller than that measured by Motohashi *et al.* It is possible that the larger hysteresis which the authors report was the result of defects in the powder samples or uncompensated spins at grain boundaries.

A broad hump in the susceptibility is evident at around  $285 \pm 5$  K for all sample orientations and at all applied magnetic fields. This temperature corresponds roughly to the onset of the low-temperature splitting of a phonon mode at  $\nu \sim 550 \text{ cm}^{-1}$ , as observed in IR conductivity measurements (not shown). This suggests that this feature in the susceptibility arises from a structural phase transition intrinsic to  $\text{Na}_{0.8}\text{CoO}_2$ , rather than from an impurity phase such as CoO (an antiferromagnet with  $T_N=292$  K). This interpretation is consistent with our muon spin rotation ( $\mu\text{SR}$ ) measurements, which exhibit no traces of CoO (see below). The origin of the structural transition remains to be determined.

The specific heat  $C_p$  also exhibits a sharp anomaly at  $19.8 \pm 0.1$  K, which indicates the onset of long-range antiferromagnetic ordering (Fig. 2). The entropy contained in this anomaly amounts to  $0.08(1)$  J/mol K and corresponds to about 10% of the entropy of the  $\text{Co}^{4+}$  spin-1/2 system. There is a slight excess heat capacity above  $T_N$ , extending up to  $\sim 35$  K. These observations are consistent with the short-range magnetic fluctuations above  $T_N$  visible in the

magnetic-susceptibility measurements. The specific heat at low temperatures contains a contribution linear in temperature which is revealed in a  $C_p/T = \gamma + \beta T^2$  plot (inset in Fig. 2). It is slightly sample dependent and amounts to  $8.4(3)$  and  $10.4(4)$  mJ/mol  $\text{K}^2$  for the two measured crystals. We ascribe it to the Sommerfeld term from the conduction electrons. If the cubic term  $\beta$  is attributed to the contribution of acoustic phonons alone (ignoring possible contributions from magnons), it corresponds to a Debye temperature of  $\sim 420$  K.

$\mu\text{SR}$  experiments were performed using the GPS setup at the  $\pi\text{m}3$  beam line at the Paul-Scherrer-Institute (PSI) in Villigen, Switzerland, which provides 100% spin-polarized muons. The  $\mu\text{SR}$  technique is especially suited for the investigation of magnetic materials with small magnetic moments. In particular, it allows one to study the homogeneity of the magnetic state on a microscopic scale, and also to access its volume fraction. The accessible time scale is  $10^{-6}$ – $10^{-10}$  s. Details about the  $\mu\text{SR}$  technique can be found in Ref. 13.

Figure 3(a) shows  $\mu\text{SR}$  spectra obtained in a zero-field configuration. The total asymmetry of the polarization function was normalized using a measurement done in a weak transverse field of 100 Oe at 50 K, with the sample in the paramagnetic state. Spectra at 7.5 K for two different orientations of the muon spin polarization with respect to the crystallographic  $c$  axis are shown. It is evident that the spectra contain several oscillating components, which means that the muons experience several well-defined local magnetic fields. We analyzed the spectra at 7.5 K using a relaxation function of the form

$$P(t) = P(0) \sum_i A_i \cos(2\pi \nu_\mu^i t) \exp(-\lambda^i t). \quad (1)$$

A good description was obtained using a sum of three oscillatory terms with frequencies and relaxation rates (at low temperature) of  $\nu_\mu = 1.25, 2.6,$  and  $3.2$  MHz and  $\lambda = 0.8, 1.2,$  and  $2.8 \mu\text{s}^{-1}$ , plus one nonoscillatory term with a very small relaxation rate of  $\lambda = 0.02 \mu\text{s}^{-1}$ , which accounts for the component of the muon spin parallel to the internal fields [lines in Fig. 3(a)]. The amplitudes  $A_i$  of the oscillating (nonoscillating) components are proportional to  $\sin^2\Phi$  ( $\cos^2\Phi$ ), where  $\Phi$  is the angle between the initial muon spin direction and the local magnetic field at the muon site.<sup>13</sup> A detailed analysis of the angular dependence will be reported in a forthcoming publication. We note here only that the amplitudes of the components with  $\nu_\mu = 1.25, 2.6,$  and  $3.2$  MHz have a ratio close to 3:2:1 and account for the full  $\mu\text{SR}$  asymmetry, which means that essentially all of the muons experience a finite and well-defined local magnetic field. In other words, the static magnetic order below  $T_N = 19.8$  K involves the entire sample volume. This conclusion is supported by the very small nonoscillatory component in the spectrum at  $\Theta = 60^\circ$ , as well as by our weak-transverse-field measurements (not shown here), in which the oscillatory component corresponding to the applied magnetic field of  $H^{ext} = 100$  Oe vanishes below  $T_N$ . The  $\mu\text{SR}$  data also establish that the magnetic order disappears rapidly above  $T_N = 19.8$  K. The spectrum at 25 K is already well described by

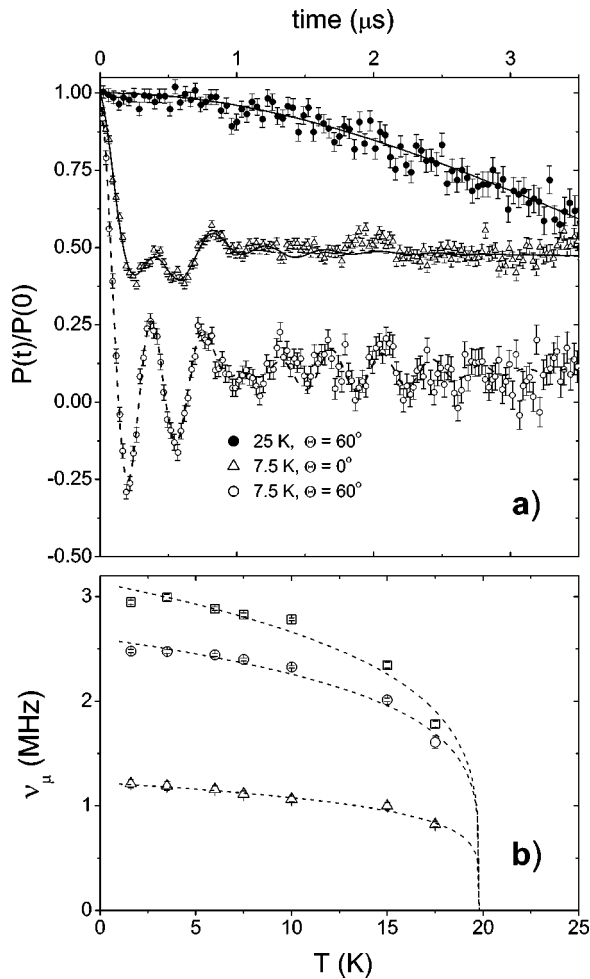


FIG. 3. (a) Time dependence of the spin polarization of muons implanted in a  $\text{Na}_{0.82}\text{CoO}_2$  crystal in zero field at  $T = 7.5$  K.  $\Theta$  is the angle subtended by the initial spin polarization and the crystallographic  $c$  axis. The lines are the results of fits described in the text. (b) Temperature dependence of the  $\mu\text{SR}$  frequencies extracted from the  $P(t)$  spectra [panel (a)]. The dashed lines are guides to the eye.

a so-called Kubo-Toyabe function with a small relaxation rate of  $0.17 \mu\text{s}^{-1}$ , which can be accounted for by the internal fields due to the Co nuclear magnetic moments.

Evidence for antiferromagnetic ordering in  $\text{Na}_x\text{CoO}_2$  was obtained in a previous  $\mu\text{SR}$  study by Sugiyama *et al.*<sup>14</sup> While the Néel temperatures we find are in good agreement with these data, there are other substantial differences between our results. First, they obtained much smaller volume fractions of the magnetically ordered phase (about 20% in their polycrystalline  $\text{Na}_{0.75}\text{CoO}_2$  sample and 50% in their  $\text{Na}_{0.9}\text{CoO}_2$  single crystal). This suggests that their samples might have been less homogeneous, possibly due to an inhomogeneous Na content. Intercalation of water may also constitute an important difference. This is known to occur rather rapidly under moist conditions, especially for powder samples. Second, the magnitude and number of the deduced muon spin-precession frequencies are rather different. In their polycrystalline samples, they also observe three muon frequencies, at about 3.3, 2.6, and 2.1 MHz. However, their

relative amplitudes are different from those observed in our crystals, so that, for instance, the largest contribution comes from the highest-frequency mode. In their single-crystal sample, they observe only one frequency, though there is some evidence for the existence of at least one additional frequency.<sup>14</sup>

This leaves us with the important question of whether the different local magnetic fields are a consequence of different crystallographic muon stopping sites, or whether they should be interpreted in terms of different magnetic environments. The latter may be caused by commensurate magnetic order with a large unit cell, but could also arise from a macroscopically inhomogeneous magnetic state. As noted by Sugiyama *et al.*, the local fields experienced by the muons in different crystallographic muon sites should be principally of dipolar origin. Potential muon stopping sites are close to the oxygen ions and near Na(1) or Na(2) vacancies. We performed a calculation of the dipolar fields for the case of Co moments directed along the  $c$  axis and exhibiting A-type antiferromagnetic order. We find that the magnetic fields near the Na(1) and the Na(2) vacancies are vanishingly small. We therefore suggest that the muons are located primarily near the oxygen ions, forming a myoxyl bond as that seen in other oxide compounds, such as the high- $T_c$  cuprate superconductors.<sup>15</sup> Assuming an ordered moment of  $0.3\mu_B$ , we obtain a local magnetic field of about 2 MHz at the oxygen site.

The three different muon spin-precession frequencies observed in the experiment could be due to the presence of a structural minority phase with a monoclinic distortion, as discussed in Ref. 2. However, if a minority phase were present in our sample, its Néel temperature would have to be very similar to that of the majority phase. This conclusion is based on the temperature dependence of the local magnetic fields, which is shown in Fig. 3(b). It is evident that all three local fields exhibit a similar  $T$  dependence and disappear above the magnetic transition at 19.8 K evident in the magnetization and the specific-heat data. In this context, it is also important to note that the absence of a fast-relaxing component in the spectrum at 25 K proves that the sample does not contain a significant amount of the most common magnetic impurities, such as  $\text{Co}_3\text{O}_4$  ( $T_N = 33$  K) or  $\text{CoO}$ .

It is also possible that the three frequencies reflect a commensurate spin order in which the same local field is re-

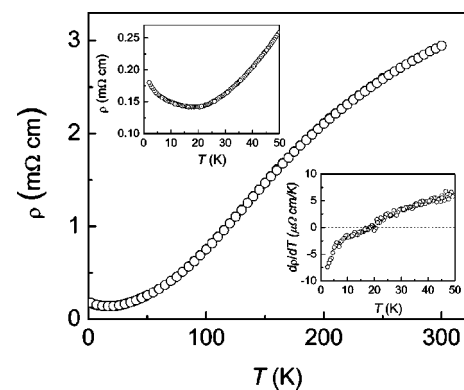


FIG. 4. In-plane resistivity of  $\text{Na}_{0.82}\text{CoO}_2$ . Insets: Low-temperature resistivity and its temperature derivative.

peated in every third crystallographic unit cell. However, our data do not support an interpretation in terms of an incommensurate magnetic order,<sup>14</sup> which should give rise to much larger depolarization rates and to a different form of the relaxation function. We have tried fitting with Bessel functions, but could not obtain a reasonable fit. Since  $\mu$ SR data provide only local information, it is not straightforward to deduce further information concerning the magnetic ordering pattern. Neutron-scattering experiments will be required to settle this important issue.

Figure 4 shows the in-plane resistivity measured on a rectangular crystal ( $4 \times 3 \times 0.6$  mm<sup>3</sup>) with a four-point ac technique ( $\nu = 119$  Hz). The resistivity is frequency independent between 19 and 1000 Hz and exhibits metallic character for  $T > T_N$ , with a residual-resistivity ratio  $\rho(300 \text{ K})/\rho(4.2 \text{ K}) \sim 20$ . The temperature derivative of the resistivity changes sign at  $T_N$  (insets in Fig. 4). This is the

behavior expected if a spin-density wave opens a small gap at the Fermi surface. Mikami *et al.* observe a similar upturn in resistivity measurements on the  $\alpha$  phase (with  $x = 0.90$ ).<sup>11</sup>

In conclusion, we have observed an antiferromagnetic state with Néel temperature  $T_N = 19.8 \pm 0.1$  K and an ordered moment perpendicular to the CoO<sub>2</sub> layers. The susceptibility exhibits a broad peak around 30 K, characteristic of two-dimensional antiferromagnetic fluctuations.  $\mu$ SR measurements confirm that the static magnetic order encompasses nearly 100% of the volume. The in-plane resistivity shows a minimum around the magnetic phase transition. Our findings are consistent with an intrinsic, commensurate antiferromagnetic spin-density wave transition at 19.8 K, and are incompatible with incommensurate magnetic order.

We acknowledge the technical support of A. Amato at the PSI and of E. Brücher and G. Siegle at the MPI.

- 
- <sup>1</sup>K. Takada, H. Sakurai, E. Takayama-Muromachi, F. Izumi, R.A. Dilanian, and T. Sasaki, *Nature (London)* **422**, 53 (2003).
- <sup>2</sup>C. Fouassier, G. Matejka, J.-M. Reau, and P. Hagenmuller, *J. Solid State Chem.* **6**, 532 (1973).
- <sup>3</sup>M. Jansen and R. Hoppe, *Z. Anorg. Allg. Chem.* **408**, 104 (1974).
- <sup>4</sup>R.J. Balsys and R.L. Davis, *Solid State Ionics* **93**, 279 (1996).
- <sup>5</sup>T. Tanaka, S. Nakamura, and S. Iida, *Jpn. J. Appl. Phys., Part 2* **33**, L581 (1994).
- <sup>6</sup>Y. Wang, N.S. Rogado, R.J. Cava, and N.P. Ong, *Nature (London)* **423**, 425 (2003).
- <sup>7</sup>I. Terasaki, Y. Sasago, and K. Uchinokura, *Phys. Rev. B* **56**, R12685 (1997).
- <sup>8</sup>T. Motohashi, E. Naujalis, R. Ueda, K. Isawa, M. Karppinen, and H. Yamauchi, *Appl. Phys. Lett.* **79**, 1480 (2001).
- <sup>9</sup>D. P. Chen, H. C. Chen, A. Maljuk, A. Kulakov, H. Zhang, and C. T. Lin (unpublished).
- <sup>10</sup>P. Lemmens, V. Gnezdilov, N. N. Kovaleva, K. Y. Choi, H. Sakurai, E. Takayama-Muromachi, K. Takada, T. Sasaki, F. C. Chou, C. T. Lin, and B. Keimer, *J. Phys.: Condens. Matter* **16**, S857 (2004).
- <sup>11</sup>M. Mikami, M. Yoshimura, Y. Mori, T. Sasaki, R. Funahashi, and M. Shikano, *Jpn. J. Appl. Phys., Part 1* **42**, 7383 (2003).
- <sup>12</sup>T. Motohashi, R. Ueda, E. Naujalis, T. Tojo, I. Terasaki, T. Atake, M. Karppinen, and H. Yamauchi, *Phys. Rev. B* **67**, 064406 (2003).
- <sup>13</sup>See, for example, A. Schenck, *Muon Spin Rotation: Principles and Applications in Solid State Physics* (Adam Hilger, Bristol, 1986).
- <sup>14</sup>J. Sugiyama, H. Itahara, J.H. Brewer, E.J. Ansaldo, T. Motohashi, M. Karppinen, and H. Yamauchi, *Phys. Rev. B* **67**, 214420 (2003); J. Sugiyama, J.H. Brewer, E.J. Ansaldo, B. Hitti, M. Mikami, and Y.M.T. Sasaki, cond-mat/0310637 (unpublished).
- <sup>15</sup>M. Weber, P. Birrer, F.N. Gygax, B. Hitti, E. Lippelt, H. Maletta, and A. Schenck, *Hyperfine Interact.* **63**, 207 (1990); N. Nishida and H. Miyatake, *ibid.* **63**, 183 (1990).